ROCK PHYSICS MODELING TO CONSTRAIN PETROPHYSICAL PROPERTIES IN THE PRODUCTIVE ZONE OF THE MARCELLUS SHALE, WV FROM WIRELINE LOG DATA

Sharif M. Morshed

Department of Geological Sciences
The University of Texas at Austin

ABSTRACT

A rock physics characterization based on wireline log data is proposed for constraining the petrophysical properties of the productive interval in the Marcellus Shale. The method involves two parts, 1) petrophysical interpretation of organic shale from wireline log data, and 2) rock physics modeling utilizing the interpreted log data. A petrophysical interpretation of the more radioactive interval of log data suggests that higher TOC is associated with lower clay content. This interpretation also showed that upper the part of the Marcellus Shale is clay dominated whereas the lower part is quartz dominated. The productive interval did not contain significant amount of pyrite or carbonate minerals. Following the interpreted petrophysical data, the rock physics modeling was performed using differential effective medium (DEM) scheme in an inclusion based model to estimate the effective elastic moduli of the composites. The elastic moduli of the matrix phase in the DEM were provided with the Voigt-Reuss-Hill average for a composition of quartz and clay. Imbedded inclusions were assumed. Three types of inclusion phases were considered; a dry pore (i.e. equant pores or ellipsoidal pores), a water-wet clay pore and kerogen. Dry pores were saturated with pore fluids simulating reservoir situations with the low frequency Gassmann equations. Rock physics modeling suggests that the elastic properties of the Marcellus Shale were controlled by the interplay of clay content, kerogen content and low aspect ratio pores. Low aspect ratio pores (~1/40) also comprise the dominant pore types in the Marcellus Shale and these pores are more common in the lower part of the formation. This proposed rock physics scheme constrains the dominant petrophysical properties to be applied for surface seismic data interpretation.

INTRODUCTION

The Devonian Marcellus Shale of West Virginia is a well-known organic rich mudrock. The structure of the Marcellus formation can be mapped with surface seismic data. Its productive interval can be easily recognized by very high gamma response (>400 API) in borehole log data. Many drilled wells in West Virginia, however results in non-commercial production. Therefore,

it is a central issue to link lithologic and petrophysical properties with the elastic (i.e. seismic) properties. Like any other organic plays, quantification of critical factors such as suitability of hydraulic fracturing and volume of TOC are essential. Suitability of hydraulic fracturing may relate to the lithology, lithofacies and pore types. Therefore, it is important to understand the underlying relation between seismic parameters with the variation in lithology, lithofacies, TOC and pore type. A wide variety of pore types in mudrocks are sometimes seen in thin section and SEM images (Loucks et al., 2012). This variety of pore type makes the problem more complex when considering pores such as clay, microcrack, fracture, organic and inter-particle may exist. These pores may vary widely in size and shape. It is known that low aspect ratio pores may have considerable effect on seismic velocity. However, the seismic response to a complex pore system mentioned earlier has not been thoroughly studied. In this study, I address lithology, TOC and pore type in a rock physics model to understand the elastic properties of the Marcellus Shale from well log data.

DATA

Wireline log and kerogen content analysis data from one well in West Virginia were used in this project. Figure 1 shows wireline log data including P-wave velocity, S-wave velocity, fast and slow shear slowness (dipole S1 and S2), gamma ray, photoelectric factor (PE), density and resistivity. The productive interval is highlighted with light yellow color. This shale gas interval can be easily identified by very low Thorium to Uranium ratio in addition to very high GR response (>300 GAPI). The Uranium response usually increases with the increase of organic matter (OM) and Th is associated with clay minerals (Fertl and Chilingar, 1988). Therefore, low TH/U ratio may relate to high organic content with low clay content. All resistivity (shallow and deep) values on the order of 10^3 in a clastic sequence may indicate resistive components such as OM and gas may present in the formation. Density porosity and neutron porosity are corrected for a shaley-sand matrix as shown in the Figure 1. However, discrepancies between neutron porosity and density porosity shows two distinct zones, i.e. higher differences in the upper part and lower differences in lower part of the highlighted Marcellus Shale interval.

METHOD

The method involves two steps. In the first step, a suite of conventional wireline log data was interpreted for lithology, TOC and porosity. Interpreted data was used in the second part for rock physics modeling of the Marcellus Shale. After the modeling, the lithofacies and petrophysical properties of the Marcellus shale were linked to the sensitive seismic parameters. A brief outline

of the workflow is shown in Figure 2. The wireline log data were interpreted for lithologies, porosity and pore types. Then, several effective medium schemes were applied to obtain the elastic properties of the rock using the interpreted lithology and porosity data. Finally, results from the effective medium schemes were compared with the observed log data and to check for errors and inconsistencies. The mineral properties used for the study (Mavko et al., 2009) are given in Table 1.

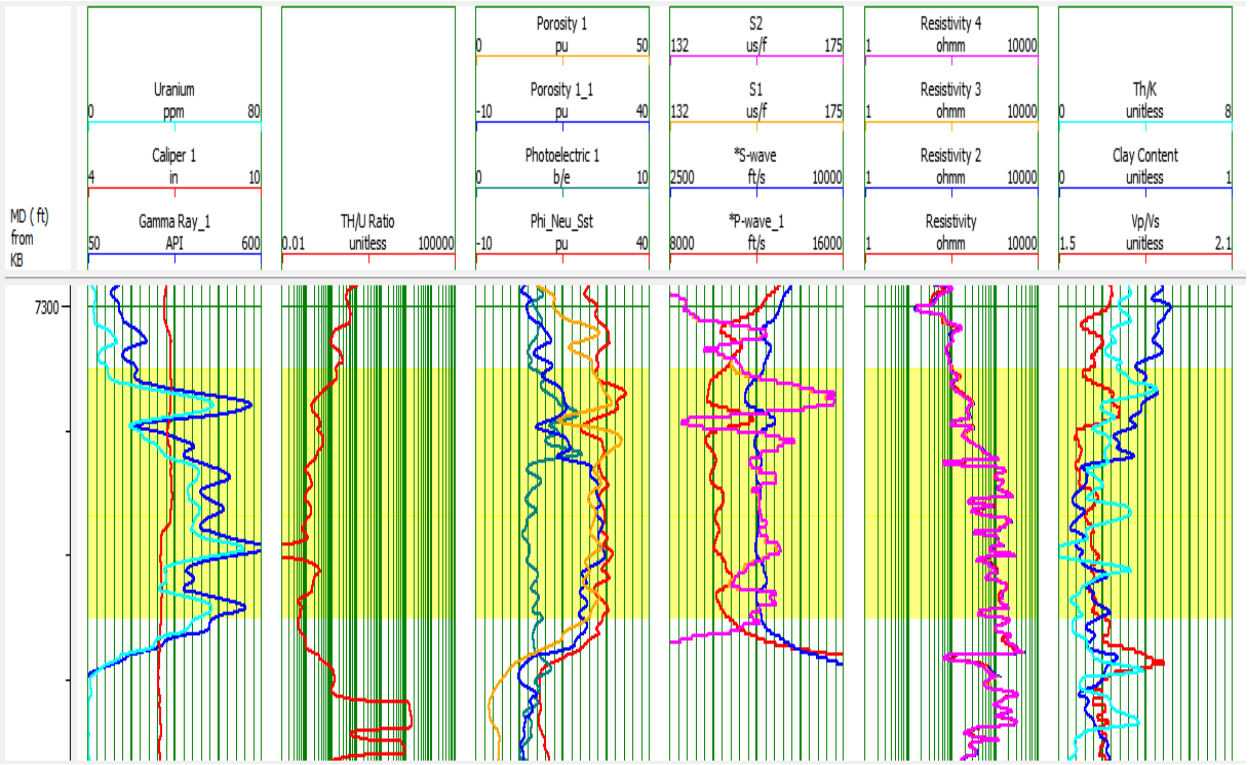

Figure 1. Wireline log data including gamma ray, Thorium/ Uranium ratio (Th/U), density porosity (porosity1_1), sonic porosity (porosity_1), neutron porosity, photoelectric factor, P and S wave velocities, Thorium/ Potassium ratio (Th/K) and resistivity logs of Cather-04 well from West Virginia. The organic shale interval is highlighted by yellow color. Because S1 and S2 shear slownesses are almost same (i.e. no HTI anisotropy), S1 slowness cannot be seen. Resistivity logs are numbered according to the radial depth of investigation (i.e. resistivity 4 is the deepest). A very low Th/U ratio (plotted on a log scale) and high resistivity are particularly noticeable in the Shale gas formation. All seismic velocities also decrease in the selected interval.

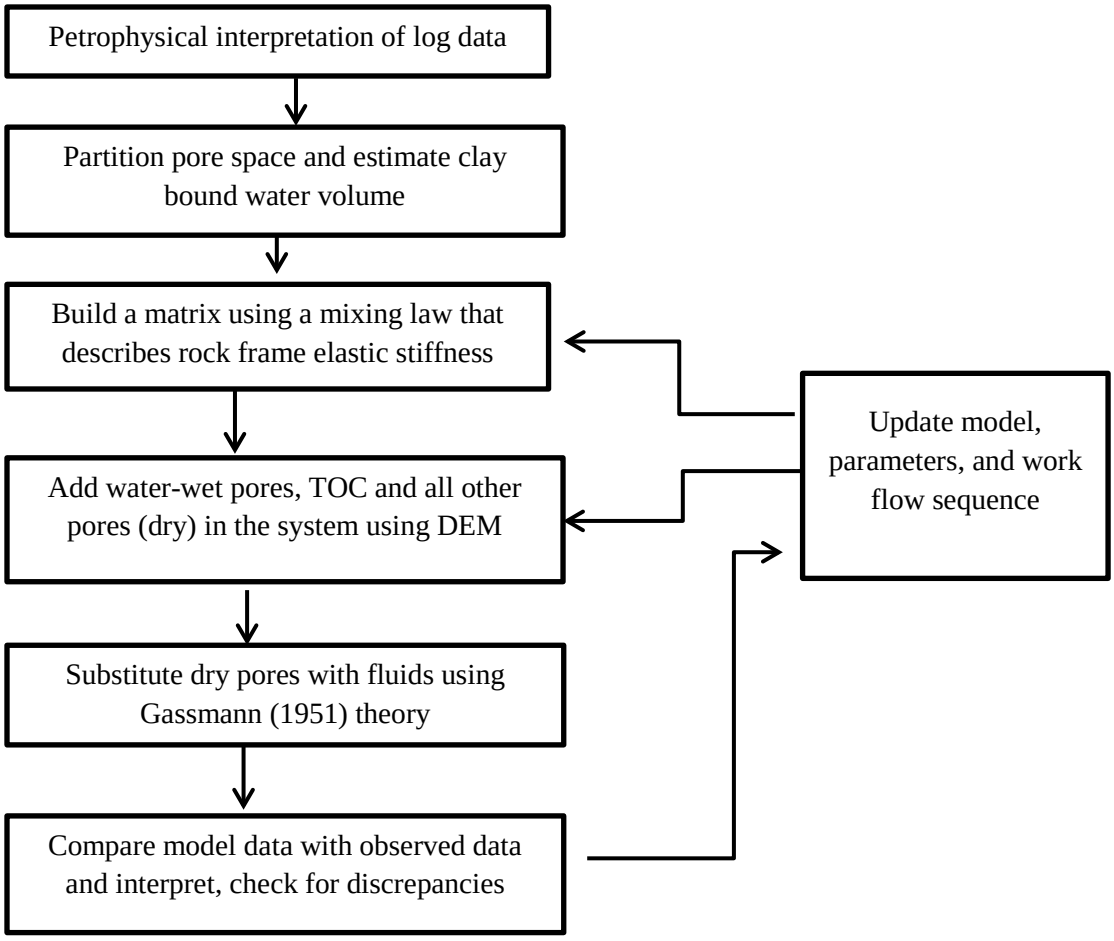

Figure 2. A schematic workflow of the project. Rock physics modeling using DEM constitutes the central part. Input data to DEM was provided by petrophysical interpretation of log data. Background matrix moduli in the DEM were estimated by mixing laws. Kerogen and pores were incorporated in the DEM as inclusions.

Lithology Interpretation from log data

Organic shale lithology can be highly variable. Wang (2012) studied data from 707 wells along with XRD (X-ray diffraction) and PNS (pulsed neutron spectroscopy) data of the Marcellus Shale of WV. He found that Marcellus Shale mineralogy varies highly in quartz, illite, chlorite, kerogen, feldspar and pyrite. Here pyrite has very different properties in density, PE, elastic moduli and resistivity. Therefore, if pyrite effect is not properly corrected, log interpretation can be problematic. However, pyrite has high PE value (18 b/e) and high density (4.93 g/cc), therefore PE-density cross plot can identify Pyrite affecting data. However, most data show much lower density (<2.58g/cc) and lower PE (<6 b/e) to have any major amount of Pyrite (<5 %) (Figure 3). Therefore, log data were not corrected for pyrite. After checking for

pyrite, the spectral GR data were plotted on a TH-K plot to identify the dominant clay mineral type (Figure 4). Most of the data fall in the illite domain which also agrees with all previous works on the Marcellus Shale.

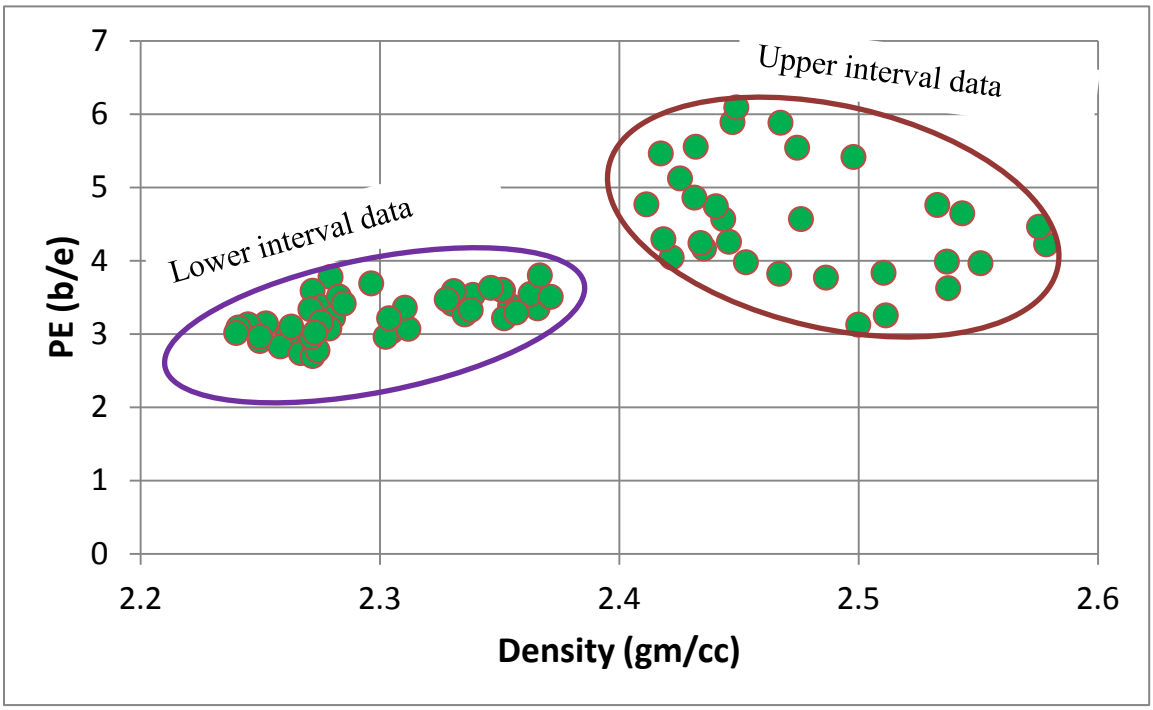

Figure 3. Log data is plotted on the PE-density cross plot. Plot shows that maximum density is 2.58 g/cc and maximum PE is 6. Therefore, pyrite which has high density (4.93 g/cc) and high PE (18 b/e) may not present in a significant quantities. However, data are separated out in two domains (circled in the figure), which may translates quartz rich domain and illite-rich clay domain.

After confirming that lithofacies of the selected log interval do not contain any major mineralogy other than quartz, clay and kerogen, these constituents can be quantitatively interpreted in the following ways. First, both density porosity and neutron porosity can be corrected for quartz matrix. Then, the volume of clay in the solid fraction of the rock is interpreted using the following equation:

$$V_{clay} = (N_{\phi} - D_{\phi}) / (N_{\phi(sh)} - D_{\phi(sh)}), \quad (1)$$

where, N_{ϕ}= Neutron Porosity (assuming shaly sand Matrix)

D_{ϕ}= Density Porosity (assuming shaly sand Matrix)

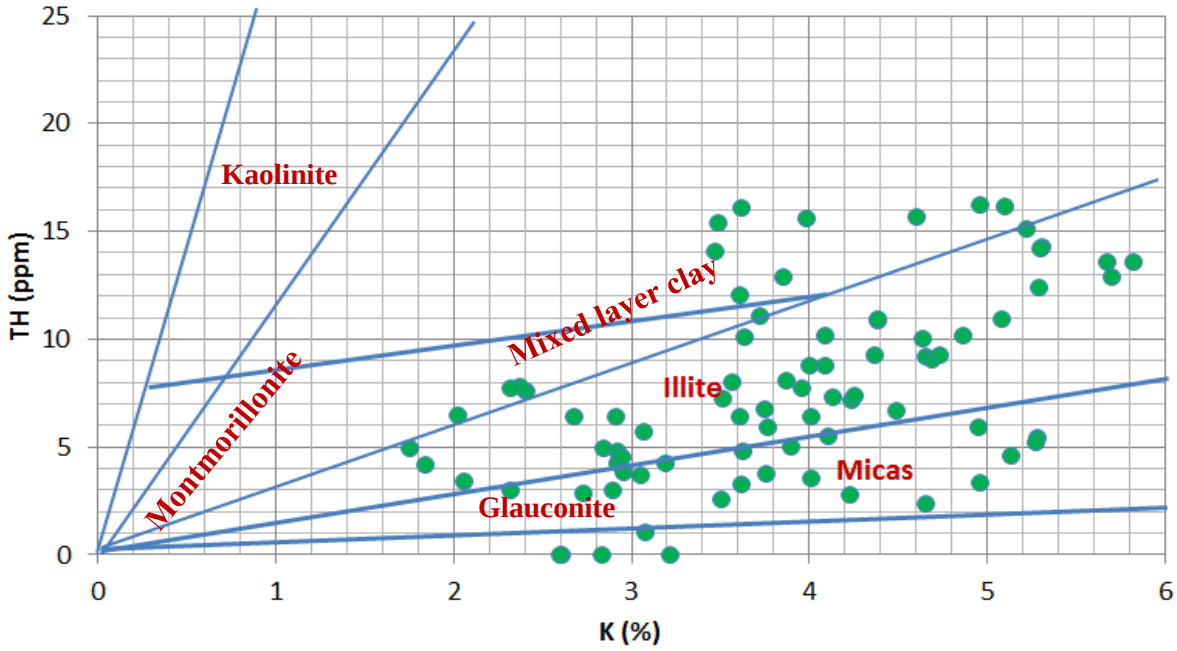

Figure 4. Log data is plotted on the Slb Lith-2 plot. Plot shows that most of the data is concentrated on the Illite zone.

$N_{\phi(sh)}$-= Neutron Porosity at pure Shale

$D_{\phi(sh)}$)= Density Porosity at pure Shale

If core data, XRD, ECS or PNS log data are available at any point of the selected interval, then the Vclay value can be corrected and normalized. In the absence of the above mentioned measurement, a pure shale point can be taken as the point that shows the maximum difference between neutron porosity and density, and high TH/K ratio. Basically, neutron porosity H ions, and H ion is present both in formation fluid , kerogen and Clay mineral. The density porosity also sees kerogen as pores because of the low density of Kerogen (0.6 g/cc – 1.5 g/cc).

Porosity estimation

The total volume of kerogen and pores can be estimated by the following equations,

$$(k+\phi_t) = (\rho_{matrix} - \rho_{log}) / (\rho_{matrix} - \rho_f) \quad (2)$$

Where k is the kerogen content and ϕ_t is the total porosity. p_f is the density of the pore fluid taken as constant 1.05gm/cc regarding the fact that density tool mostly senses the mud filtrate. It was also assumed that the density of kerogen is close to the density of the pore fluid. The matrix

density (ρ_{matrix}) was taken as 2.71 g/cc to account for the specific siliciclastic rock which contains mainly quartz (density 2.65 g/cc) and clay where the dominant clay mineral is illite (2.78 g/cc). It was also assumed that the rock contains other minor (<5%) heavier minerals like calcite (2.71 g/cc) and pyrite (4.93 g/cc).

TOC estimation

There are several methods proposed in the literature for estimation of TOC utilizing spectral GR (i.e., Th/U ratio), density porosity, resistivity, sonic porosity and PE data. However, density is one of the most common log, and I used the method that Myers and Jenkyns (1992) proposed to estimate TOC form density log by the following equations,

$$TOC\ (\%) = \frac{0.85*\rho_k\ *\phi_{fl}}{\rho_k\ *\phi_{fl}+\rho_{ma}*(1-\phi_{fl}-\phi_k)} \quad (3)$$

where, $\phi_{fl} = \frac{\rho_{ns}-\rho_{ma}}{\rho_{fl}-\rho_{ma}}$, $\phi_k = \frac{\rho_s-\rho_{ns}}{\rho_k-\rho_{ma}}$

Where, ρ_{ns} =Density reading at the vertically adjacent shale interval which doesn't contain kerogen (averaged a value from the log)
ρ_s =Density reading at the productive interval
ρ_{ma} =2.71 g/cc , assumed matrix density
ρ_k =1.3 g/cc , assumed kerogen density
ρ_{fl} =1.05 g/cc, density of brine
ϕ_{fl} =Water filled porosity
ϕ_k=Kerogen filled porosity

Pore partitioning

An important step for this study was to partition the pore. Pore partitioning was done in the same fashion as in Xu et al (2012). It includes five components that comprise the pore system, such that

$$\phi_t = \phi_{Clay} + \phi_{IP} + \phi_{MC} + \phi_{Equant} + \phi_{Fracture} \quad (4)$$

Here, ϕ_t, ϕ_{Clay}, ϕ_{IP}, ϕ_{MC}, ϕ_{Equant} and $\phi_{Fracture}$ represent total porosity, clay porosity, interparticle porosity, equant porosity and fracture porosity respectively. In addition to these five pore types, organic pores can also be included.

Clay porosity was estimated using the following equation,

$$\phi_{Clay} = V_{sh} * \phi_{sh} \quad (5)$$

Here, V_{sh} is the volume of clay content and ϕ_{sh} is the density porosity at pure shale sequence in the log interval which was 0.11. For estimating fracture porosity dipole log and FMI log can be used. However, there were no differences in S1 and S2 in the dipole sonic log data (Figure 1) and no indication of vertical fractures in FMI log data, therefore $\Phi_{Fracture}$ was set to zero. I also disregarded separating microcrack porosity, and included it in the interparticle porosity. The interparticle porosity was taken as, $\phi_{IP} = \phi_t - \phi_{Clay} - \phi_{toc}$. Figure 5 shows the result of the petrophysical interpretation along with clay porosity.

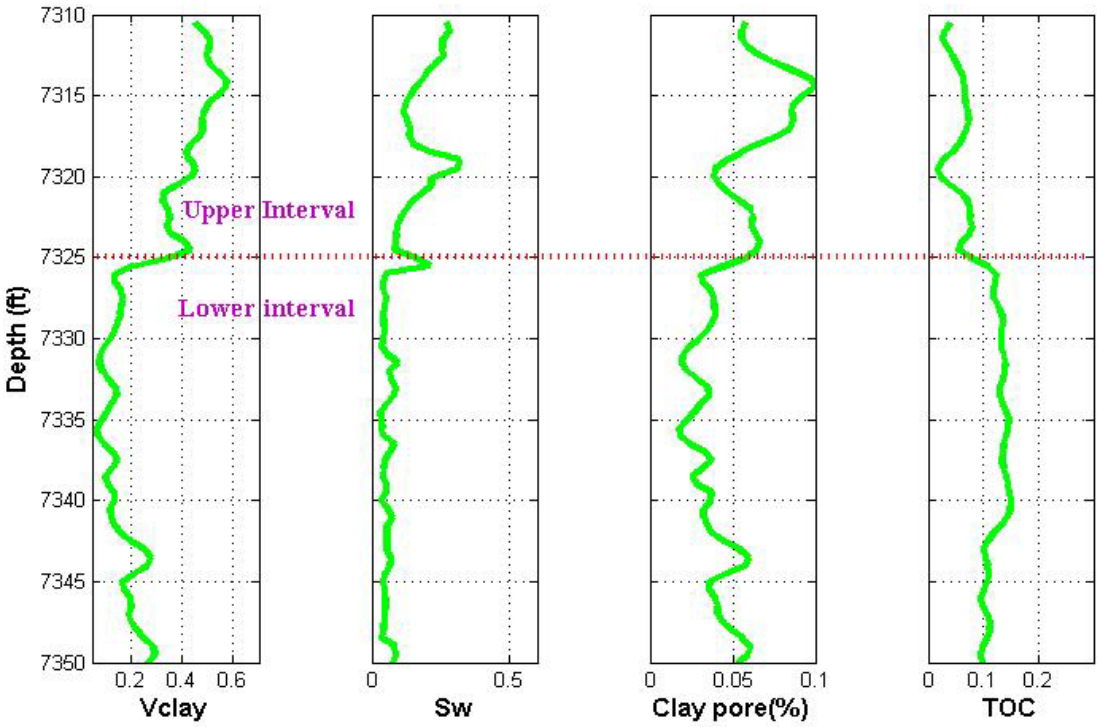

Figure 5. Interpreted clay content (V_{clay}), water saturation (S_w), clay pore and TOC (%) from the log data in the soft productive interval. The dotted line separates two distinct intervals mainly for variation in clay content. The lower interval (7325-7350 ft) also contains higher TOC and lower Sw which translates that this interval is more promising for hydrocarbons than the upper interval.

Table 1. Moduli and densities of minerals used in this study (Mavko et al., 2009).

	Bulk modulus (GPa)	Shear modulus (GPa)	Density (g/cc)
Quartz	36.6	45	2.65
Clay	25	8	2.7
Kerogen	2.9	2.7	1.3
Brine	2.4	0	1.02
Gas	0.07	0	0.2

Differential Effective Medium Model (DEM)

DEM is an inclusion based model for a two-phase composite where inclusions are added incrementally to the matrix phase (phase 1) (Cleary et al., 1980; Norris, 1985; Zimmerman, 1991). The matrix phase is the host material and the effective moduli depend on the construction path taken to reach the final composite. The isotropic formulation for effective bulk (K*) and shear moduli (K*) are given in a coupled system of ordinary differential equations as, (Berryman, 1992)

$$(1-y)\frac{d}{dy}[K^*(y)] = (K_2 - K^*)P^{(*)}(y)$$

$$(1-y)\frac{d}{dy}[\mu^*(y)] = (\mu_2 - \mu^*)Q^{(*)}(y) \quad (6)$$

Initially, K*(0)=K1, and μ*(0)=μ1, where K1 and μ1 are the bulk and shear moduli of the matrix material, K2 and μ2 are the bulk and shear moduli of the inclusion material, and y is the concentration of the inclusion material. $P^{(*)}$ and $Q^{(*)}$ are the geometric factors that depend on inclusion shapes. The system of equations can be solved by Runge-Kutta 4^{th} order method for ordinary differential equations. In DEM, taking material 1 as the host and material 2 as the inclusion will not result the same effective properties as taking material 2 as the host even if the final concentrations are same in both cases. The original model was given for isolated inclusions i.e. the elastic frame stays connected until the inclusions form total volume. Therefore, critical porosity (Nur et al., 1991) which defines the boundary between the load bearing phase and suspension phase was introduced in the DEM by Mukerji et al. (1995). Mukerji et al. (1995) proposed that the moduli of the critical phase can be estimated by a Reuss (1929) average of the end members. Moyano et al. (2012) disclosed that threshold porosities (i.e. critical porosity) are mainly controlled by aspect ratios of the inclusions.

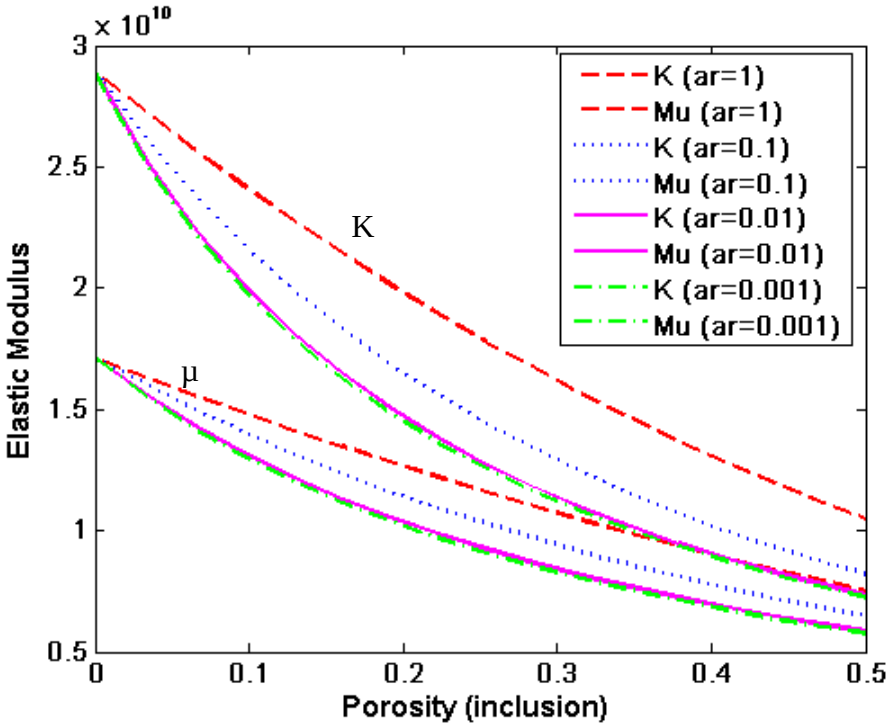

Figure 6. An illustration of the DEM scheme for understanding the effect of inclusion moduli and inclusion shape to host material. Here, the host is a solid rock of 40% Quartz with clay, and kerogen is the inclusion. It shows that aspect ratio of kerogen inclusion plays a significant role in this scheme; lower aspect ratio produces much lower elastic moduli than high aspect ratios.

A general illustration of the effect of the incrementally added inclusion and inclusion shape on host the material is shown in Figure 6. The matrix is a solid rock of 40% quartz with clay, and the inclusion is a kerogen. The critical porosity was taken as 0.5. It is found that low aspect ratio pores on the order of ~1/40 reduced the bulk moduli 17% more than the equant pores (ar = 1).

Bounds and Mixing laws

One way to evaluate and estimate the isotropic elastic moduli of the observed data is through theoretical bounds and mixing laws. Widely used bounds are Voigt upper bound, Reuss lower bound and Hashin-Strikman-Walpole bound. They all are based on isotropic linear elasticity and assume simple geometric arrangements of constituent grains and pores. The Hashin-Strikman-Walpole bound gives the narrowest possible range for mixtures of more than two phases. The Hashin-Strikman-Walpole bound is given as (Mavko et al., 2009),

$$K^{HS+} = \Lambda(\mu_{max}), \qquad K^{HS-} = \Lambda(\mu_{min}),$$

$$\mu^{HS+} = \Gamma(\zeta(K_{max}, \mu_{max}))\ ,\ \mu^{HS-} = \Gamma(\zeta(K_{min}, \mu_{min})) \tag{7}$$

$$\Lambda(z) = \left\langle \frac{1}{K(r)+\frac{4}{3}z} \right\rangle^{-1} - \frac{4}{3}z,\ \Gamma(z) = \left\langle \frac{1}{\mu(r)+z} \right\rangle^{-1} - z,\ \zeta(K,\mu) = \frac{\mu}{6}\left(\frac{9K+8\mu}{K+2\mu}\right)$$

Where K and μ are the bulk and shear modulus of individual phases and the brackets $\langle . \rangle$ indicate averages weighted by their volumetric proportions. Upper bounds corresponds to '+' and lower bound to '-'. The Voigt upper bound of effective elastic modulus is

$$M_v = \sum_{i=1}^{N} f_i\, M_i, \tag{8}$$

where f_i is the volume fraction of the i-th phase and M_i is the elastic modulus of the i-th phase. The Reuss lower bound is given as

$$\frac{1}{M_R} = \sum_{i=1}^{N} \frac{f_i}{M_i} \tag{9}$$

The Voigt-Reuss-Hill average is simply the arithmetic average of the Voigt upper bound and Reuss lower bound. The average is expressed as

$$M_{VRH} = \frac{M_V + M_R}{2} \tag{10}$$

Gassmann (1951) fluid substitution equations

Gassmann (1951) equations for different pore fluid cases were given for very low frequency situations where pore pressures have enough time to equilibrate throughout the pore space. The Gassmann (1951) method which is also widely applied by investigators in the field to predict different fluid scenario cases. Gassmann (1951) relations for fluid substitution in isotropic rocks can be stated as (Mavko and Bandyopadhyay, 2009),

$$K_{sat} = K_m\left(\frac{K_{dry}+Q}{K_m+Q}\right) \tag{11}$$

$$\text{Where, } Q = \frac{K_{fl}}{\phi}\left(\frac{K_m - K_{dry}}{K_m - K_{fl}}\right)$$

with $\mu_{sat} = \mu_{dry.}$ Here K_{dry}, K_{sat}, K_m, and K_{fl} are the bulk moduli of the dry rock, the saturated rock, the solid mineral, and the saturating pore fluid, respectively. The shear moduli of the dry rock and the saturated rock are μ_{dry} and μ_{sat}. The Gassmann (1951) equations assume a

homogeneous mineral modulus and statistical isotropy of the pore space, but it is free of assumption about pore geometry (Mavko et al., 2009).

MODELING RESULTS AND DISCUSSION

Petrophysical analysis of the log data shows that highly radioactive interval of the Marcellus Shale mainly contains illitic clay with quartz. The illitic clay signature was confirmed through Th/K ratio, density and PE factor readings (Figure 1, 3 and 4). The very low TH/U ratio along with high resistivity indicates high TOC. Log interpreted results are shown in Figure 5. The lower part of the studied interval seems more promising for exploration as it contains more TOC. The lower interval also contains more quartz which is known to make the rock more brittle than clay does. Therefore, high quartz may indicate comparatively better zone for hydraulic fracturing.

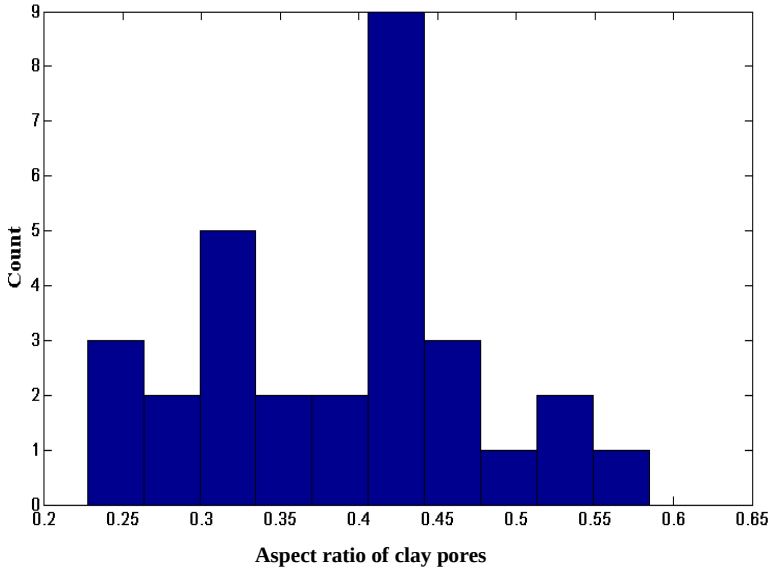

Figure 7. Histogram of Aspect ratios of the clay pores.

The interpreted petrophysical data were used for rock physics modeling. Figure 2 shows the work flow. I used Voigt-Reuss-Hill average to estimate the elastic moduli of the solid matrix to be used in the DEM model. Only quartz and clay composites were considered for the matrix. Clay volume was taken from the log interpreted data. Elastic properties of the mineral for the model are given in Table 1, critical porosity was considered 0.4. Figure 7, 8(a) and 8(b) shows the distribution of aspect ratios for clay pores, TOC and interparticle pores, respectively.

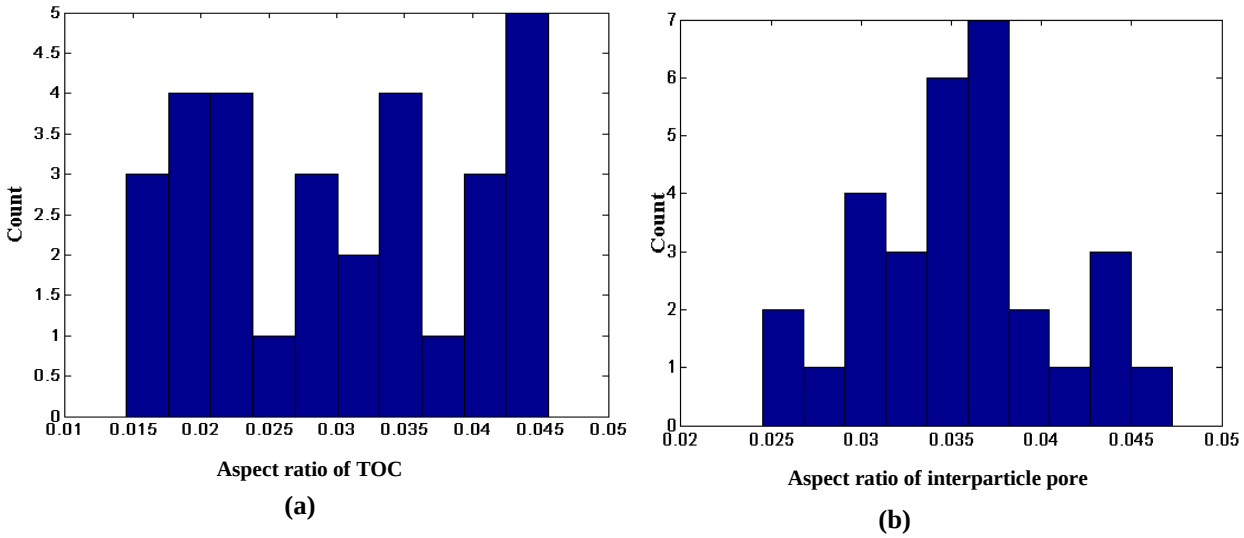

Figure 8. Histogram of Aspect ratios of the Kerogen masses (a) and the interparticle pores (b).

Figure 9 (a) and 9 (b) shows the results of the modeling with the observed log data. The lower part (below 7325 ft) (Figure 9(a)) of the Marcellus shale shows reasonable good match between the observed log data and modeled data. However, the upper part (7310-7325 ft) shows some deviation between the modeled data and observed data. Therefore, a trial and error method was applied and it was found that the upper part of the Marcellus is elastically soft and matrix moduli can be best approximated by Reuss bound. After using the Reuss bound with everything else (i.e. lithology, TOC, aspect ratio) left the same, the modeling seems better fit with the log data (Figure 9(b)). Finally, model data along with observed data are compared with theoretical bounds (Figure 10 (a) and (b)), and found that both of them falls between the upper and lower limits. The theoretical bounds were plotted for a constant kerogen content while changing the clay and quartz content. 15 % and 60 % clay content were considered, therefore quartz content were 77% and 32% respectively. With the modeled parameter, shear moduli gives a better match than the bulk moduli (Figure 10 (a) and (b)). For the bulk moduli, some of the observed data seems less stiff than the modeled data. However, the modeled data is within the theoretical limits for the interpreted mineralogical volume fractions. Therefore, kerogen, clay as well as low aspect ratio pores dominantly control the elastic properties of the productive interval of the Marcellus Shale. Anisotropy was not taken account for the modeling. So, anisotropic modeling is the next step for future work.

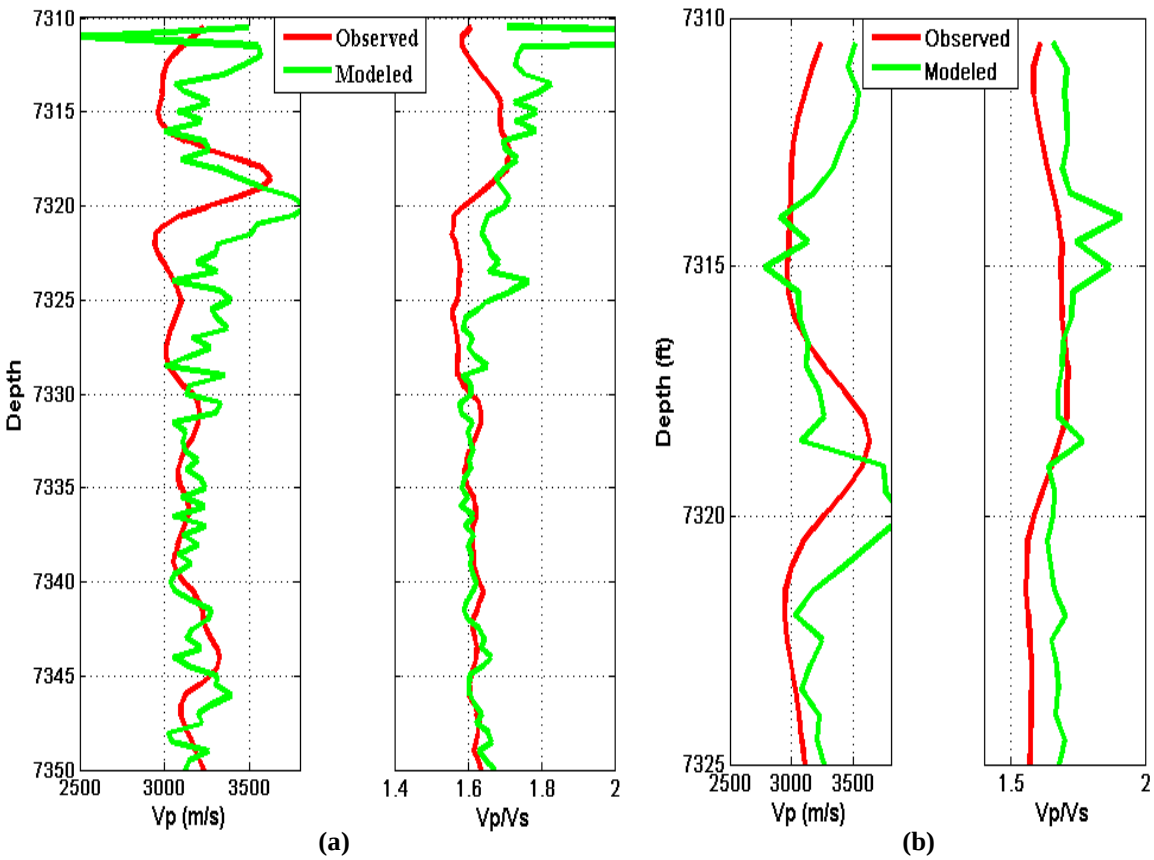

Figure 9. Final model data with the observed data in the productive interval. (a) Shows the result for the total productive interval (7310-7350 ft) for the case when matrix moduli in the DEM was provided using Voigt-Reuss-Hills average from the log interpreted mineralogical concentrations (i.e., Quartz, Clay, TOC). (b) Shows the result for the upper productive interval (7310-7325 ft) for the case when matrix moduli in the DEM was provided using Reuss average using the same mineralogical concentrations. It is clear that some part of upper interval (7310-7350 ft) is elastically softer than the lower interval, though the lower interval contains more TOC.

CONCLUSIONS

The petrophysical analysis and rock physics modeling of the higher radioactive interval of the Marcellus shale suggests that the studied zone contains variable amounts of illitic clay which is related with variable elastic (i.e., seismic) properties. The rock contains higher amount of quartz and TOC in the lower part of the productive interval which translates that the lower part (25ft) of the productive interval is a better productive zone. Overall, the rock is soft and it contains low aspect ratio pores with bedding parallel, sub-parallel kerogen masses. The three factors such as clay, kerogen and pore types dominantly control the elastic properties of the productive interval.

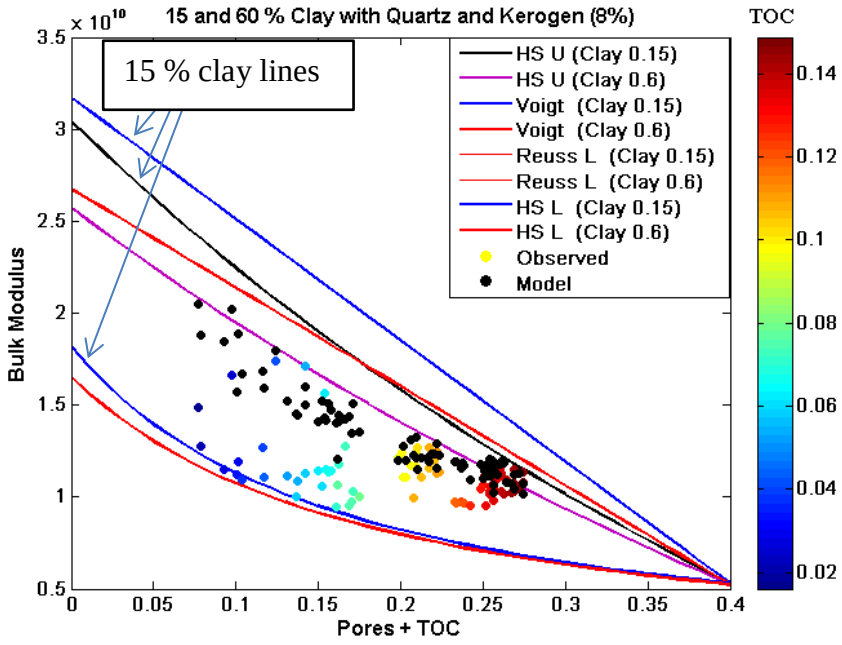

(a)

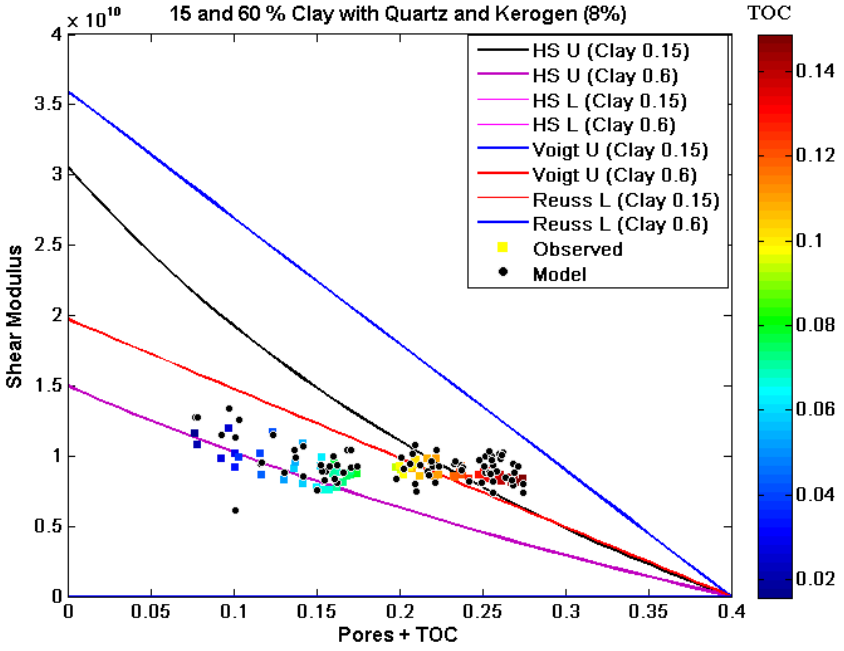

(b)

Figure 10. Theoretical bounding lines along with observed and model data for bulk moduli (a) and shear moduli (b). Bound lines are plotted for two cases; 15% clay and 8% TOC with Quartz, and 60% Clay and 8% TOC with Quartz. Hashin-Strikman lower bound seemed overlapped with Reuss bounds. The observed data are color coded by TOC content. Both observed and model data seems to fall with in theoretical bounds.

ACKNOWLEDGEMENTS

The EDGER forum at the University of Texas at Austin supported this project. The author also would like to thank Petroedge Resources for providing data.

REFERENCES

Berryman, J.G., 1992b. Single-scattering approximations for coefficients in Biot's equations of poroelasticity. J. Acoust. Soc. Am., 91, 551–571.

Cleary, M.P., Chen, I.-W., and Lee, S.-M., 1980. Self-consistent techniques for heterogeneous media. Am. Soc. Civil Eng. J. Eng. Mech., 106, 861–887.

Fertl, H. F and Chilingar, V. G., 1988, Total organic carbon content determined from well logs, SPE Formation Evaluation, **3**, 407-419

Gassmann, F., 1951, Über die Elastizität poröser Medien: Vierteljahrsschrift der Naturforschenden Gesellschaft in Zurich, 96, 1–23.

Loucks, R.G., Reed R. M., Ruppel S.C., and Hammes U., 2012, Spectrum of pore types and networks in mudrocks and a descriptive classification for matrix related mudrocks pores, AAPG Bulletin, V. 96, N0.6 , pp 1071-1098

Mavko, G., and K. Bandyopadhyay, 2009, Approximate fluid substitution for vertical velocities in weakly anisotropic VTI rocks: Geophysics, 74, D1-D6.

Mavko, G., T. Mukerji, J. Dvorkin, 2009, The rock physics handbook, tools for seismic analysis of porous media: Cambridge University Press.

Mukerji, T., Berryman, J.G., Mavko, G., and Berge, P.A., 1995a. Differential effective medium modeling of rock elastic moduli with critical porosity constraints. Geophys. Res. Lett., 22, 555–558.

Moyano, B., Spikes, K.T., Johansen, T. A., and Mondol, N.H., 2012, Modeling compaction effects on the elastic properties of clay water composites. Geophysics, 77 (5), D171-D183.

Myers, K.J. and Jenkyns, K.F. (1992) Determining total organic carbon contents from well logs: an intercomparison of GST data and a new density log method. Geological applications of wireline logs II, P-F. geol. Soc. London Spec. Publ. 65, 369-376.

Norris, A.N., 1985. A differential scheme for the effective moduli of composites. Mech. Mater., 4, 1–16.

Nur, A., Mavko, G., Dvorkin, J., and Gal, D., 1995. Critical porosity: the key to relating physical properties to porosity in rocks. In Proc. 65th Ann. Int. Meeting, Soc. Expl. Geophys., vol. 878. Tulsa, OK: Society of Exploration Geophysicists.

Reuss, A., 1929. Berechnung der Fliessgrenzen vonMischkristallen aufGrund der Plastizita¨tsbedingung fu¨r Einkristalle. Z. Ang. Math. Mech., 9, 49–58.

Wang, G., 2012, Black Shale lithofacies prediction and distribution pattern analysis of Middle Devonian Marcellus Shale in the Appalachian basin, Northeastern U.S.A., PhD Dissertation, West Virginia University.

Xu, S., and Chen G., 2012, Rock Physics model for simulating seismic response in layered fractured rocks, US patent 8184502B2

Zimmerman, R.W., 1991. Compressibility of Sandstones. New York: Elsevier.